Synthesis of a carbon nanobelt

Guillaume Povie,[1,2,3] Yasutomo Segawa,[1,2,*] Taishi Nishihara,[1,2] Yuhei Miyauchi,[1,2,4] Kenichiro Itami[1,2,3,5,*]

Affiliations:

[1] JST-ERATO, Itami Molecular Nanocarbon Project, Chikusa, Nagoya 464-8602, Japan.

[2] Graduate School of Science, Nagoya University, Chikusa, Nagoya 464-8602, Japan.

[3] Integrated Research Consortium on Chemical Sciences, Nagoya University, Japan.

[4] Institute of Advanced Energy, Kyoto University, Uji, Kyoto, 611-0011, Japan.

[5] Institute of Transformative Bio-Molecules (WPI-ITbM), Nagoya University, Chikusa, Nagoya 464-8602, Japan.

*Correspondence to: itami@chem.nagoya-u.ac.jp (KI), ysegawa@nagoya-u.jp (YS)

Abstract:

The synthesis of a carbon nanobelt, comprising a closed loop of fully fused edge-sharing benzene rings, has been an elusive goal in organic chemistry for over 60 years. Here we report the synthesis of one such compound through iterative Wittig reactions followed by a nickel-mediated aryl-aryl coupling reaction. The cylindrical shape of its belt structure was confirmed by x-ray crystallography, and its fundamental optoelectronic properties were elucidated by ultraviolet-visible absorption, fluorescence, and Raman spectroscopic studies, as well as theoretical calculations. This molecule could potentially serve as a seed for the preparation of structurally well-defined carbon nanotubes.

One Sentence Summary:

Here we report the first chemical synthesis of a carbon nanobelt, a belt-shaped compound consisting solely of fused benzene rings.

Main Text:

Belt-shaped compounds consisting solely of fused benzene rings, or carbon nanobelts, were proposed as potentially game-changing molecules in chemistry (Fig. 1A) (*1*,*2*) even before the discovery of carbon nanotubes (CNTs) in 1991 (*3*). For example, cyclacene, the shortest belt segment of zigzag CNTs, appeared in the literature in 1954 as a hypothetical molecule for theoretical study (*4*). Although Stoddart (*5*), Schlüter (*6*), Cory (*7*), our group (*8*) and others have targeted cyclacene and its derivatives, synthetic attempts toward such zigzag nanobelts have failed (*1*,*2*). In parallel to these campaigns, Vögtle proposed an armchair nanobelt (also known as

a Vögtle belt), representing a segment of armchair CNTs, and initiated studies into the synthesis of this structure in the 1980s (*9*). Inspired by this goal set by Vögtle, many groups including Herges (*10*), Iyoda (*11*), Bodwell (*12*) and Scott (*13*) have described extensive efforts to access various armchair nanobelts, but none have succeeded. Unlike these fully fused, edge-sharing carbon nanobelts, the chemistry of carbon nanorings (arenes linked by single bonds) has bloomed in recent years (Fig. 1B) (*14*). Cycloparaphenylenes (CPPs) were first synthesized in 2008, and since then, a number of CPP-related carbon nanorings, including potential precursors to carbon nanobelts, have been synthesized by Jasti, Yamago, Isobe, Müllen, our group and many others (*14*). However, attempts to convert those precursors into carbon nanobelts have been thwarted, mainly by strain-relieving rearrangement reactions (*15*). Iyoda's group came closest to isolating a carbon nanobelt in their observation of the mass peak of [10]cyclophenacene upon laser irradiation of a *Z*-ethenylene-bridged macrocycle (Fig. 1C) (*11*). Using a distinct strategy, Scott has succeeded in the synthesis of a CNT end-cap (*16*), and Nakamura (*17*) and Gan (*18*) extracted the substructures of nanobelts by multiaddition reactions to C_{60} or C_{70}, respectively (Fig. 1D).

Building upon the knowledge, strategies, and methods accumulated during the above-mentioned extensive efforts, we herein report the bottom-up synthesis and isolation of carbon nanobelt **1** (Fig. 2). This compound represents a belt segment of (6,6)CNT and is an isomer of [12]cyclophenacene. The strain energy of **1** (119.5 kcal·mol^{-1}) estimated by DFT calculation (see Supplementary Materials (SM) for details) is almost the same as that of [12]cyclophenacene (115.1 kcal·mol^{-1}) (*19*). The synthetic route to **1** (Fig. 2) consisted of sequential Wittig reactions for the construction of the key macrocycle **2** and a subsequent nickel(0)-mediated aryl-aryl coupling reaction. This route was inspired by Iyoda's extensive studies of the all-*Z*-benzannulenes (*11*) and Stępień's synthesis of strained π-systems (*20*).

The synthesis started with benzylic bromide **3** and aldehyde **4**, both of which were easily prepared in four steps from *p*-xylene (see SM). A Wittig reaction then provided stilbene **5** with high *Z*-selectivity (*Z/E* 20:1) owing to the *ortho*-bromo effect (*21*). Without isolation, **5** was subjected to a subsequent monodebromination (*22*) in the same pot to afford **6** in 80% yield from **3** after recrystallization. Repeating the same reaction sequence with **6** and **4** worked efficiently to furnish the trimer **7** with similar yields. Phosphonium formation followed by deprotection of dimethyl acetal with HCl produced the bifunctional unit **8**, which, after counterion exchange, could be recrystallized in excellent yields as a PF_6 salt. Treatment of a CH_2Cl_2 solution of **8** with *t*-BuOK triggered a sequential cyclodimerization. The resulting macrocycle **2** could be isolated in multigram quantities after recrystallization from toluene, and the all-*Z* macrocyclic structure was unambiguously established by x-ray crystallography.

With precursor **2** in hand, we investigated the key aryl-aryl coupling reaction. Among the various conditions tested, the combination of $Ni(cod)_2$ and 2,2'-bipyridyl with a short reaction time furnished **1**. Under the optimal conditions, which required 12 equivalents of $Ni(cod)_2$ and 2,2'-bipyridyl at 70 °C for 15 minutes, pure **1** could be isolated as red crystals in 1% yield. Although this low yield leaves room for considerable improvement, the ability to prepare precursor **2** on large scale permitted sufficient quantities of this long-sought carbon nanobelt **1** to be purified, isolated and fully characterized. NMR analysis revealed two and four sets of non-equivalent protons and carbons, respectively, in accord with the D_{3d} symmetry of the molecule. The signals were attributed based on 2D-NMR experiments and were in good agreement with calculated values (see SM for details).

The structure of **1** was confirmed by x-ray crystallography (Fig. 3). Suitable crystals generated from a *N*,*N*'-dimethylpropyleneurea/$CHCl_3$/cyclohexane solution at room temperature gave a reliable x-ray crystal structure of **1** [R_1 = 0.0399 ($I>2\sigma(I)$] as **1**·3$CHCl_3$. As shown in Fig. 3A and 3B, **1** has a belt-shaped structure (C_{2h} symmetry in crystal) with a diameter of 8.324 Å in which all benzene rings are fused. This is a distinct structural feature from previously reported carbon nanorings such as CPPs (*23*).

In the packing structure, individual molecules of **1** are separated from one another by chloroform molecules localized above, below and outside **1** (Fig. 3C,D). All crystallographically independent C–C bond lengths are shown in Fig. 3E. Judging from the short lengths of the C1–C1* and C5–C9 bonds, it appears that the resonance structure assigning them double bond character (C=C is typically 1.337 Å) is the main contributor (Fig. 3F, upper structure). However, the C3–C3* and C7–C11 bonds are shorter than the bonds in [6]CPP linking the benzene rings (1.490(2) Å) (*23*), implying that ring **a** may also have weak aromatic character (Fig. 3F, lower structure) as a minor resonance structure. Ring **b** appears to be more strongly aromatic in accord with the small bond alternation around its circumference. These observations are in good agreement with the optimized structure of **1** predicted by DFT calculations. The nucleus-independent chemical shift (NICS) (*24*) values (ring **a**: –2.01, ring **b**: –7.45) also indicate substantial aromaticity of ring **b**.

For insight into the electronic structure of **1**, we investigated its photophysical properties (Fig. 4A). The optical absorption spectrum of **1** in CH_2Cl_2 solution presents two major bands at 284 and 313 nm. A smaller peak at 412 nm and a weakly absorbing region extending up to 500 nm are also observed. The absorption in the 450–500 nm region could be attributed to a symmetry-forbidden HOMO→LUMO transition (528 nm) with an oscillator strength (*f*) of 0.00 predicted by time dependent (TD)-DFT calculations at the B3LYP/6-31G(d) level of theory (Fig. 4D and also see SM). The weak absorption of the forbidden transition of **1** may be caused by structural rigidity, which prevents deformation away from high symmetry. The 412 nm absorption could be assigned to a combination of HOMO–1→LUMO and HOMO→LUMO+1 transitions, which were calculated to absorb at 413 nm with weak oscillator strength (f = 0.08). Carbon nanobelt **1** exhibits a deep red fluorescence, easily visible in solution and in the solid state (Fig. 4B,C, and also see SM). The fluorescence spectrum recorded upon excitation at 500 nm shows a broad emission band extending to the near infrared region with a maximum emission at 630 nm (Fig. 4A). Time resolved measurements revealed a particularly long-lived excited state, both in CH_2Cl_2 solution (τ = 20.6 ns) and in the crystalline form (τ = 26.8 ns). The quantum yield (Φ = 3% in CH_2Cl_2 solution), with the classical relations $\Phi = k_r \times \tau$ and $\tau = 1/(k_r + k_{nr})$, gives the rates of non-radiative and radiative decay in solution ($k_{nr} = 4.8 \times 10^7\ s^{-1}$ and $k_r = 1.5 \times 10^6\ s^{-1}$), and the latter accords with a forbidden transition

In order to compare **1** with extended CNTs, we measured the Raman spectrum of a single crystal of **1**·3$CHCl_3$ with laser excitation at 785 nm. The observed peaks were assigned to the corresponding vibration modes calculated at the B3LYP/6-31G(d) level of theory (see SM for details). Among these peaks, the frequency corresponding to the radial breathing mode was found at 261 cm^{-1}, which is closer than that of [6]CPP (231 cm^{-1}) to the 287 cm^{-1} band (*25*) seen in (6,6)CNT (*26*). These observations support the structural rigidity of nanobelt **1** and its prospective interest as a model of (6,6)CNT.

The fully fused, fully conjugated, and rigid belt structure of **1** and its unusual optoelectronic properties bode well for a range of future applications for nanoelectronics and

photonics. Just as the birth of bowl-shaped corannulene (*27*) led to a rational, controlled synthesis of C_{60} (*28*) and opened the field of geodesic polyarenes (*29*), we believe that the present synthesis of carbon nanobelt **1** could ultimately lead to the programmable synthesis of single-chirality, uniform-diameter CNTs (*30–32*) and open a field of nanobelt science and technology.

Acknowledgments:

This work was supported by the ERATO program from JST (K.I.) and the Swiss National Science Foundation (early postdoc mobility fellowship No. P2BEP2_158977 to G.P.). We thank Mr. Tsugunori Watanabe (Nagoya University) for the large-scale synthesis of **2**. Dr. Nobuhiko Mitoma (Nagoya University) is greatly acknowledged for measuring the Raman spectrum of **1**. Dr. Hideto Ito (Nagoya University) is acknowledged for assistance with quantum yield measurements and for taking photos of **1**. We thank Cathleen M. Crudden (Queen's University and Nagoya University) for fruitful discussion and critical comments. Computations were performed using Research Center for Computational Science, Okazaki, Japan. ITbM is supported by the World Premier International Research Center (WPI) Initiative, Japan. All the past and current members of the Itami group are greatly acknowledged for their support and encouragement during our decade-long campaign of ring-belt-tube projects. We dedicate this paper to the memory of Fritz Vögtle, who pioneered the carbon nanobelt research. Crystallographic data for compounds **1** and **2** are available free of charge from the Cambridge Crystallographic Data Centre under CCDC 1524455 and 1524456, respectively. These data can be obtained free of charge from the CCDC (www.ccdc.cam.ac.uk/data_request/cif).

SUPPLEMENTARY MATERIAL

www.sciencemag.org/

Materials and Methods

Fig. S1 to S19

Tables S1 to S3

References (*33–47*)

References and Notes:

1 D. Eisenberg, R. Shenhar, M. Rabinovitz, *Chem. Soc. Rev.* **39**, 2879-2890 (2010).

2 K. Tahara, Y. Tobe, *Chem. Rev.* **106**, 5274-5290 (2006).

3 S. Iijima, *Nature* **354**, 56-58 (1991).

4 E. Heilbronner, *Helv. Chim. Acta* **37**, 921-935 (1954).

5 F. H. Kohnke, A. M. Z. Slawin, J. F. Stoddart, D. J. Williams, *Angew. Chem. Int. Ed. Engl.* **26**, 892-894 (1987).

6 M. Standera, A. D. Schlüter, in *Fragments of fullerenes and carbon nanotubes*, M. A. Petrukhina, L. T. Scott, Eds. (Wiley, 2012), Ch.13.

7 R. M. Cory, C. L. McPhail, A. J. Dikmans, J. J. Vittal, *Tetrahedron Lett.* **37**, 1983-1986 (1996).

8 K. Matsui, M. Fushimi, Y. Segawa, K. Itami, *Org. Lett.* **18**, 5352-5355 (2016).

9 F. Vögtle, A. Schroder, D. Karbach, *Angew. Chem. Int. Ed. Engl.* **30**, 575-577 (1991).

10 S. Kammermeier, P. G. Jones, R. Herges, *Angew. Chem. Int. Ed. Engl.* **35**, 2669-2671 (1996).

11 M. Iyoda, Y. Kuwatani, T. Nishinaga, M. Takase, T. Nishiuchi, in *Fragments of fullerenes and carbon nanotubes*, M. A. Petrukhina, L. T. Scott, Eds. (Wiley, 2012), Ch.12.

12 B. L. Merner, L. N. Dawe, G. J. Bodwell, *Angew. Chem. Int. Ed.* **48**, 5487-5491 (2009).

13 L. T. Scott, *Angew. Chem. Int. Ed.* **42**, 4133-4135 (2003).

14 Y. Segawa, A. Yagi, K. Matsui, K. Itami, *Angew. Chem. Int. Ed.* **55**, 5136-5158 (2016).

15 F. E. Golling, M. Quernheim, M. Wagner, T. Nishiuchi, K. Müllen, *Angew. Chem. Int. Ed.* **53**, 1525-1528 (2014).

16 L. T. Scott *et al.*, *J. Am. Chem. Soc.* **134**, 107-110 (2012).

17 E. Nakamura, K. Tahara, Y. Matsuo, M. Sawamura, *J. Am. Chem. Soc.* **125**, 2834-2835 (2003).

18 Y. Li, D. Xu, L. Gan, *Angew. Chem. Int. Ed.* **55**, 2483-2487 (2016).

19 Y. Segawa, A. Yagi, H. Ito, K. Itami, *Org. Lett.* **18**, 1430-1433 (2016).

20 D. Myśliwiec, M. Stępień, *Angew. Chem. Int. Ed.* **52**, 1713-1717 (2013).

21 E. C. Dunne, É. J. Coyne, P. B. Crowley, D. G. Gilheany, *Tetrahedron Lett.* **43**, 2449-2453 (2002).

22 P. Liu, Y. Chen, Y., J. Deng, Y. Tu, *Synthesis* **2001**, 2078-2080 (2001).

23 J. Xia, R. Jasti, *Angew. Chem. Int. Ed.* **51**, 2474-2476 (2012).

24 P. v. R. Schleyer, C. Maerker, A. Dransfeld, H. Jiao, N. J. R. v. E. Hommes, *J. Am. Chem. Soc.* **118**, 6317-6318 (1996).

25 E. H. Hároz, *et al. Phys. Rev. B* **91**, 205446 (2015).

26 M. P. Alvarez, *et al. Angew. Chem. Int. Ed.* **53**, 7033-7037 (2014).

27 W. E. Barth, R. G. Lawton, *J. Am. Chem. Soc.* **88**, 380-381 (1966).

28 L. T. Scott *et al.*, *Science* **295**, 1500-1503 (2002).

29 Y.-T. Wu, J. S. Siegel, *Top. Curr. Chem.* **349**, 63-120 (2014).

30 M. F. L. De Volder, S. H. Tawfick, R. H. Baughman, A. J. Hart, *Science* **339**, 535-539 (2013).

31 J. R. Sanchez-Valencia *et al. Nature* **512**, 61-64 (2014).

32 Y. Segawa, H. Ito, K. Itami, *Nat. Rev. Mater.* **1**, 15002 (2016).

33 X. Yang, D. Liu, Q. Miao, *Angew. Chem. Int. Ed.* **53**, 6786-6790 (2014).

34 P. Ruggli, F. Brandt, *Helv. Chim. Acta* **27**, 274-291 (1944).
35 P. Liu, Y. Chen, J. Deng, Y. Tu, *Synthesis* **2001**, 2078-2080 (2001).
36 A. Altomare, et al. *J. Appl. Crystallogr.* **32**, 115-119 (1999).
37 G. Sheldrick, *Acta Crystallogr. A* **64**, 112-122 (2008).
38 K. Wakita, Yadokari-XG, Software for crystal structure analyses, 2001.
39 C. Kabuto, S. Akine, T. Nemoto, E. Kwon, *J. Cryst. Soc. Jpn.* **51**, 218-224 (2009).
40 M. J. Frisch, et al. Gaussian 09, Revision D.01, Gaussian, Inc., Wallingford CT, 2013.
41 A. D. Becke, *J. Chem. Phys.* **98**, 5648-5652 (1993).
42 C. Lee, W. Yang, R. G. Parr, *Phys. Rev. B* **37**, 785-789 (1988).
43 J. P. Merrick, D. Moran, L. Radom, *J. Phys. Chem. A* **111**, 11683-11700 (2007).
44 B. Esser, F. Rominger, R. Gleiter, *J. Am. Chem. Soc.* **130**, 6716-6717 (2008).
45 B. Hellbach, F. Rominger, R. Gleiter, *Angew. Chem. Int. Ed.* **43**, 5846-5849 (2004).
46 W. D. Neudorff, D. Lentz, M. Anibarro, A. D. Schlüter, *Chem. Eur. J.* **9**, 2745-2757 (2003).
47 E. S. Hirst, F. Wang, R. Jasti, *Org. Lett.* **13**, 6220-6223 (2011).

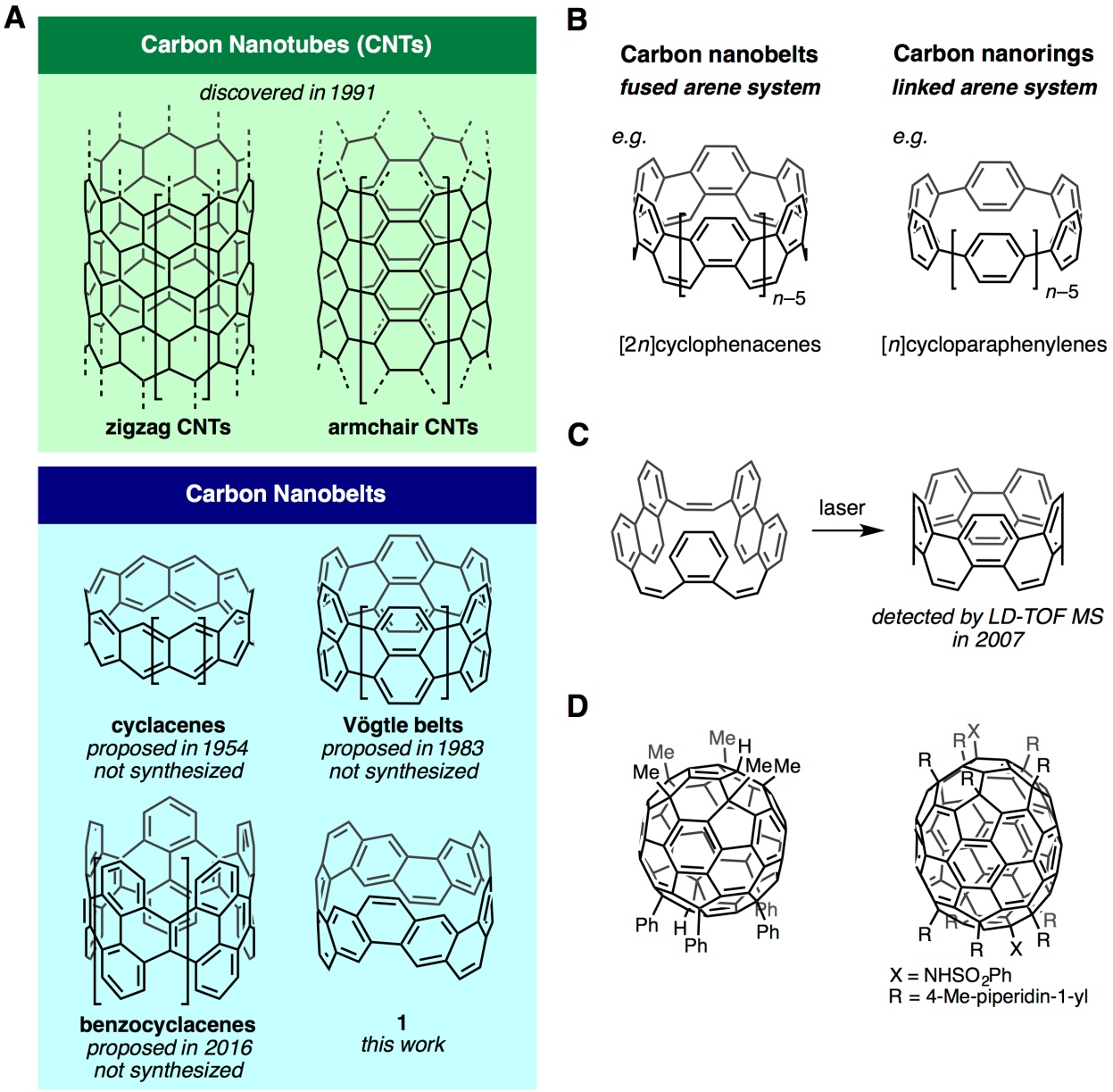

Fig. 1. Carbon nanotubes (CNTs) and carbon nanobelts. (**A**) Structures of CNTs and carbon nanobelts where the square brackets show a repeating unit. (**B**) Difference between carbon nanobelts and carbon nanorings. (**C**) Mass detection of [12]cyclophenacene by Iyoda. (**D**) Multiaddition to C_{60} and C_{70} leading to the extraction of carbon nanobelt substructures.

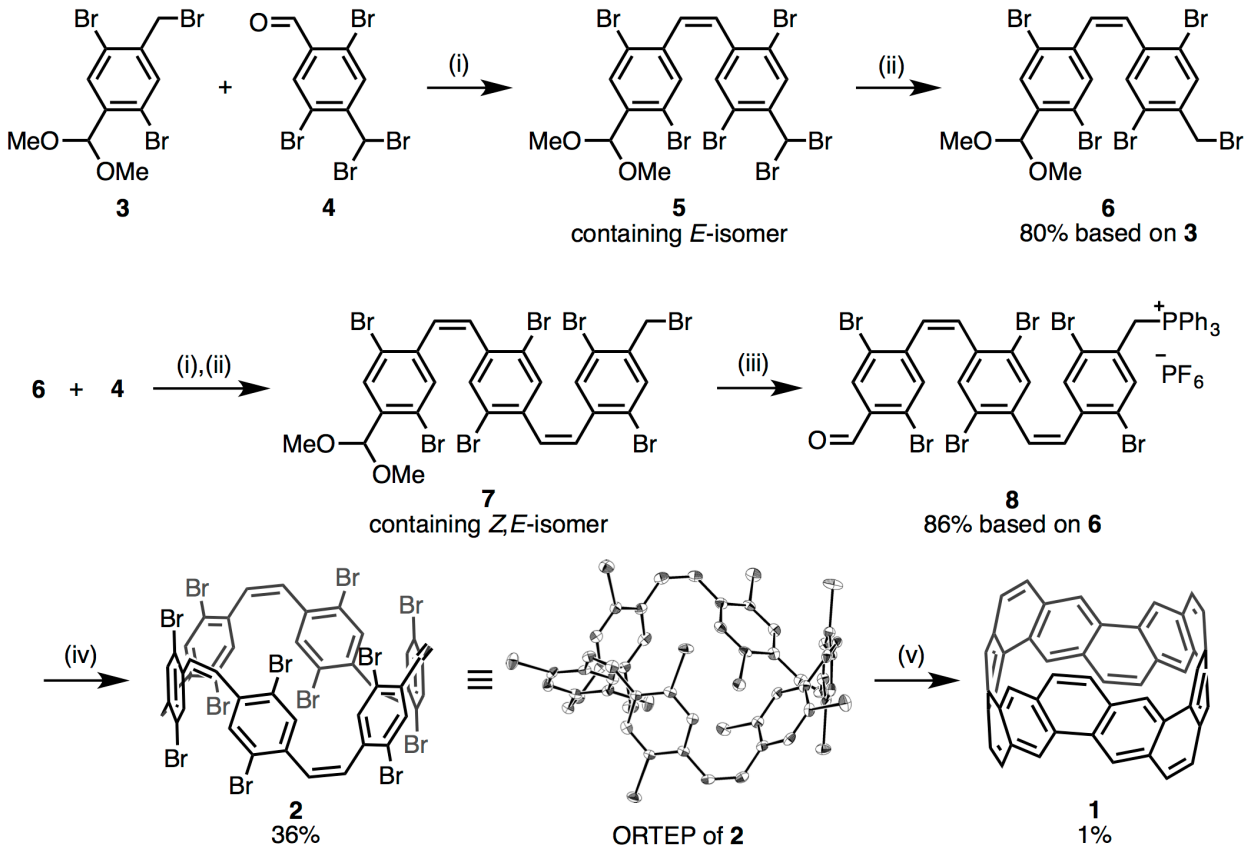

Fig. 2. Synthetic scheme to produce 1. Reaction conditions: (i) **3** or **6** (1.00 equiv), PPh_3 (1.04 equiv), THF/MeOH, reflux, 3 or 3.5 h; **4** (1.02 equiv), *t*-BuOK (1 M in THF, 1.00 equiv), room temperature (rt), 25 or 60 min. (ii) $(MeO)_2POH$ (1.30 equiv), *i*-Pr_2NEt (1.40 equiv), rt, 1 or 3 h. (iii) PPh_3 (1.04 equiv), THF/MeOH, reflux, 5 h; 4 M aq. HCl, acetone, rt, 2 h; KPF_6, CH_2Cl_2, rt, 3 min. (iv) *t*-BuOK (1 M in THF, 1.20 equiv), CH_2Cl_2, 0 °C to rt, 80 min. (v) **2** (1.00 equiv), $Ni(cod)_2$ (12.0 equiv), 2,2'-bipyridyl (12.0 equiv), DMF, 70 °C, 15 min. Abbreviations: THF = tetrahydrofuran, cod = 1,5-cyclooctadiene, DMF = *N*,*N*-dimethylformamide. Oak Ridge thermal-ellipsoid plot (ORTEP) of **2**·2toluene is shown at 50% probability, with hydrogen atoms and toluene molecules omitted for clarity.

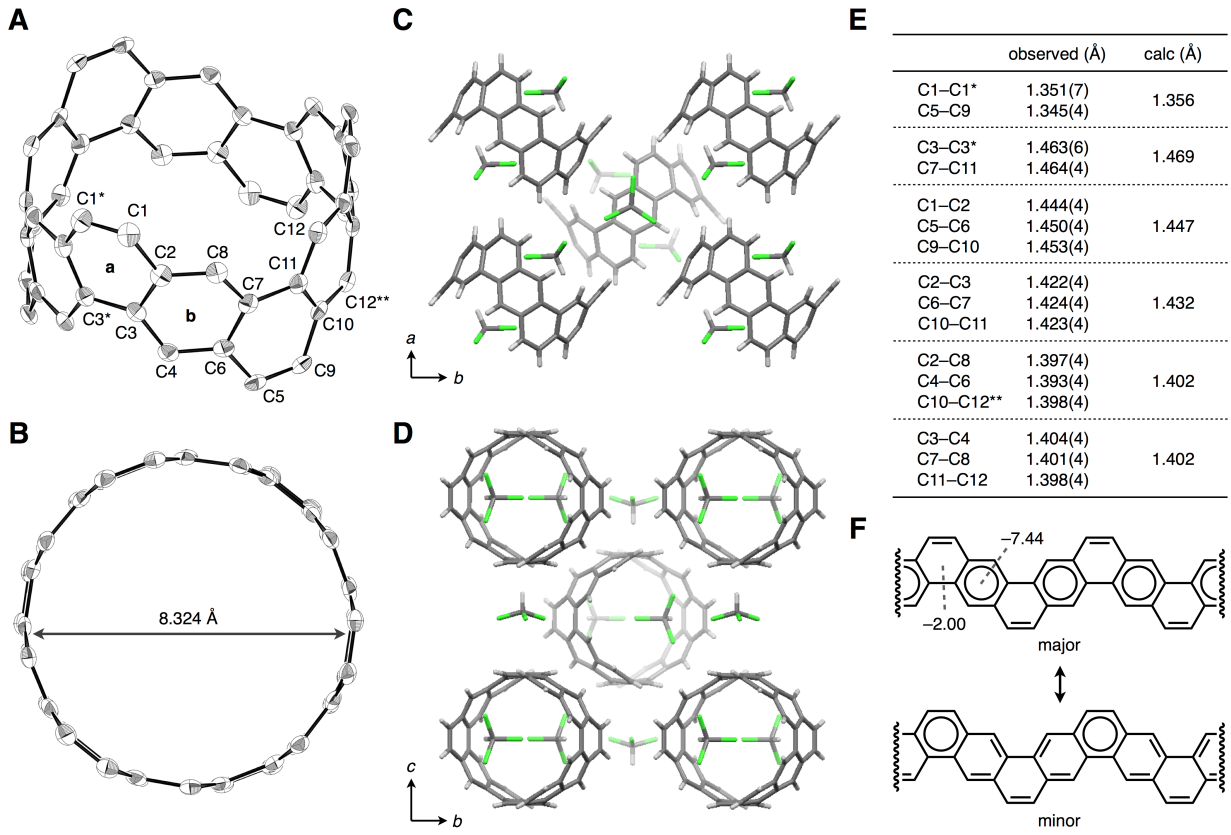

	observed (Å)	calc (Å)
C1–C1*	1.351(7)	1.356
C5–C9	1.345(4)	
C3–C3*	1.463(6)	1.469
C7–C11	1.464(4)	
C1–C2	1.444(4)	1.447
C5–C6	1.450(4)	
C9–C10	1.453(4)	
C2–C3	1.422(4)	1.432
C6–C7	1.424(4)	
C10–C11	1.423(4)	
C2–C8	1.397(4)	1.402
C4–C6	1.393(4)	
C10–C12**	1.398(4)	
C3–C4	1.404(4)	1.402
C7–C8	1.401(4)	
C11–C12	1.398(4)	

Fig. 3. Structural features of carbon nanobelt 1. (**A**,**B**) ORTEP diagram of **1**·3$CHCl_3$ at 50% probability with hydrogen atoms and solvent molecules omitted for clarity. A quarter of the entire structure constitutes an asymmetric unit; the numbers with one and two asterisks are in the second and the third asymmetric units, respectively. (**C**,**D**) Packing structures of **1** along *c* and *a* axes. One of the disordered $CHCl_3$ molecules is shown for each position. (**E**) Bond lengths of **1**. Optimization for the calculated values was performed at the B3LYP/6-31G(d) level of theory. (**F**) Resonance structures of **1** with NICS(0) values calculated at the GIAO B3LYP/6-311+G(2d,p)//B3LYP/6-31G(d) level of theory. Clar aromatic sextets are shown with circles.

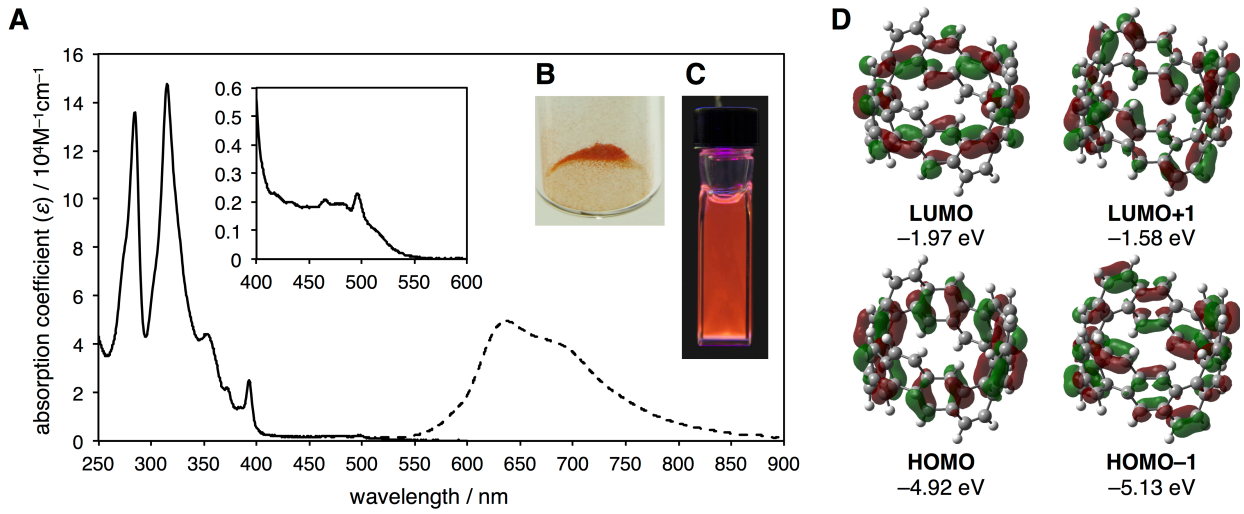

Fig. 4. Photophysical properties of carbon nanobelt 1. (**A**) UV-vis absorption (solid line) and fluorescence (broken line, normalized) spectra of the CH_2Cl_2 solution of **1**. Absorption coefficients were obtained at 5×10^{-6} M. Weakly absorbing region (inset) was measured at 7×10^{-5} M. Fluorescence spectrum was acquired following excitation at 500 nm. (**B**) Photograph of **1**·3$CHCl_3$ crystals. (**C**) Photograph of a CH_2Cl_2 solution of **1** irradiated at 365 nm. (**D**) Frontier molecular orbitals of **1** calculated at the B3LYP/6-31G(d) level of theory (isovalue = 0.003). HOMO: highest occupied molecular orbital, LUMO: lowest unoccupied molecular orbital.